Active and passive seismic monitoring of laboratory-based injection-driven fault reactivation

Veltmeijer, A.V.; Naderloo, M.; Barnhoorn, A.

DOI
10.3997/2214-4609.202310513

Publication date
2023

Document Version
Final published version

Citation (APA)
Veltmeijer, A. V., Naderloo, M., & Barnhoorn, A. (2023). *Active and passive seismic monitoring of laboratory-based injection-driven fault reactivation*. Paper presented at 84th EAGE ANNUAL Conference and Exhibition 2023, Vienna, Austria. https://doi.org/10.3997/2214-4609.202310513

2023 EAGE ANNUAL
84TH CONFERENCE & EXHIBITION
VIENNA | AUSTRIA

Active and passive seismic monitoring of laboratory-based injection-driven fault reactivation

A. Veltmeijer[1], M. Naderloo[1], A. Barnhoorn[1]

[1] Delft University of Technology

Summary

Robust and reliable prediction of (induced) earthquakes remains a challenging task. Seismicity predictions are made using probabilistic models, precursors such as average earthquake size distribution. Pore pressure variations cause stress perturbations along pre-existing fault planes in the subsurface, resulting in shear slip and seismicity. Monitoring these stress changes before fault reactivation and its resulting seismicity could greatly improve forecasting seismicity. Stress changes can be determined by changes in acoustic or seismic velocities. Therefore, experiments are performed to detect the preparatory phase of an earthquake using acoustic monitoring. Faulted sandstone samples are reactivated in the laboratory by imposing pore pressure changes by fluid injection under reservoir pressures, while continuously performing passive and active (transmission) acoustics measurements. Using coda wave interferometry (CWI) and decorrelation (K), changes in velocity and scattering are obtained before and during fault reactivation. We show that fault reactivation can be identified by a large velocity drop and an increase in K or by micro-seismic foreshocks. We show that CWI velocity change is most sensitive to both the preparatory phase and the fault reactivation. These results show acoustic monitoring of fault reactivation in the laboratory is feasible, which could improve the prediction of induced seismicity.

Active and passive seismic monitoring of laboratory-based injection-driven fault reactivation.

Introduction

Induced seismicity can pose a high risk in higher populated areas. With the increasing demand for energy and renewable energy, subsurface activities surged, which has led to an increase in recorded induced seismicity around the world. Fluid injection in the subsurface has caused many seismic events over the years. Well-known examples of injection-induced seismicity in populated areas due to pore pressure changes are the M5.4 earthquake in Pohang (South Korea), and the M3.4 earthquake in Basel (Switzerland).

Prediction of induced seismicity remains challenging, but monitoring and predicting (induced) earthquakes received much interest over the years. Seismicity predictions are made using probabilistic models (Kiraly-Proag et al., 2016), including production scenarios (Dempsey and Suckale, 2017), or are made using precursors, such as average earthquake size distribution (b-value) (Gulia et al., 2020). However, predicting seismicity remains a challenging task.

Induced seismicity often results from the reactivation of pre-existing faults. Pore pressure variations cause stress perturbations along a fault plane resulting in shear slip and seismicity. Monitoring and predicting these stress changes along the fault could greatly improve the prediction of (induced) earthquakes.

Stress changes can be determined by changes in acoustic or seismic velocities (Barnhoorn et al., 2018; Zotz-Wilson et al., 2019). A few laboratory experiments have shown precursory changes in elastic wave velocity (Kaproth and Marone, 2013; Shreedharan et al., 2020, 2021; Veltmeijer et al., 2022) and amplitude (Shreedharan et al., 2020, 2021; Veltmeijer et al., 2022) during the preparatory phase of an earthquake, however, in these studies, fault slip was not fluid-induced. Also at a larger scale, precursory signals can be observed using active acoustic monitoring. A decrease in P-wave velocity before an M6.5 in Italy was observed near the hypocentre (Chiarabba et al., 2020).

Most of the studies in the field or laboratory are based on either passive or active monitoring.

This study uses both monitoring techniques to detect the preparatory phase of an (induced) earthquake during the reactivation of faulted sandstone due to fluid injection to improve the monitoring and prediction of induced seismicity.

Methods

To monitor the fault reactivation active acoustic transmission measurements were performed throughout the experiment. The changes in velocity between two consecutive recorded waves in the obtained time series of recorded wavelets are compared using the direct S-wave arrival and coda wave interferometry (CWI) (Snieder, 2006) and coda wave decorrelation **(**CWD**) (**Larose et al., 2010) is used to monitor the changes in material scattering. The coda of the wave is set to start at two times the arrival time of the S-wave. By comparing the consecutive wavefields using a cross-correlation (CC) the variations in the medium can be assessed. The CC reaches its maximum if the travel time perturbation δt across all possible perturbed paths P is $\delta t = t_s$, for a time window of width $2t_w$ and centered around time t_k.Assuming the time shift is constant in the considered time window, the velocity change (dv/v) can be written as

$$\frac{\delta v}{v} = \frac{\delta t}{t}. \quad (1)$$

The material scattering changes, due to the addition or removal of scatter(ers), e.g. micro-fracture formation or grain crushing, in the medium and is related to the decorrelation coefficient (K) (Larose et al., 2010). By using a moving reference wavefield, the scattering medium is continuously monitored (Zotz-Wilson et al., 2019).

$$K(t_s) = 1 - CC(t_s) = 1 - \frac{\int_{t_k-t_w}^{t_k+t_w} u_{p_{j-N}}(t)\, u_{p_j}(t+t_s)\, dt}{\sqrt{\int_{t_k-t_w}^{t_k+t_w} u_{p_{j-N}}^2(t)dt \int_{t_k-t_w}^{t_k+t_w} u_{p_j}^2(t)dt}}, \quad (2)$$

where N is the number of measurements wavefield $u_{p_j}(t)$ is lagging behind the reference wavefield $u_{p_{j-N}}(t)$.

The active acoustic transmission measurements were performed using two S-wave transducers placed above and below the sample (Figure 1A), such that the waves propagate through the fault plane of the

samples. With a peak operating frequency of 1 MHz, every 2 seconds 128 S-waves were sent, recorded, and stacked to reduce the signal-to-noise ratio.
The passive acoustic (AE) monitoring to detect micro-seismic events was performed using an array of 8 piezo-ceramic transducers. The AE transducers are 5mm in diameter and directly attached to the sample, with a dominant resonant frequency of about 1 MHz, and the signals were amplified using pre-amplifiers.

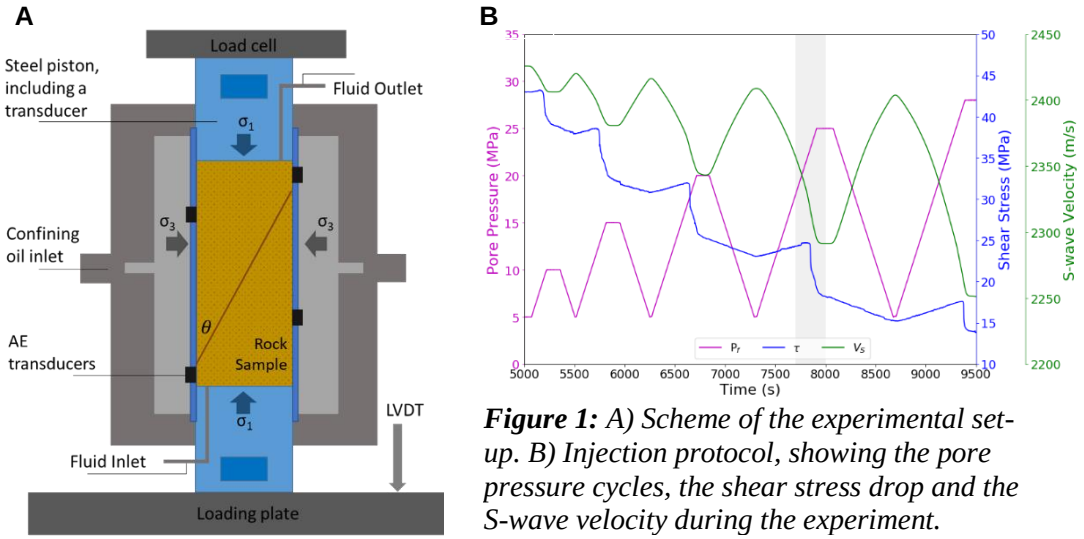

Figure 1: *A) Scheme of the experimental set-up. B) Injection protocol, showing the pore pressure cycles, the shear stress drop and the S-wave velocity during the experiment.*

The rock samples used are Red Pfaelzer sandstones, an analog of the Rotliegend sandstones of the Groningen gas reservoir (in the Netherlands), these have similar mechanical properties as the reservoir rock. The rock samples have a porosity of around 20% and dimensions of 30 ± 0.5 mm in diameter and 70 ± 2 mm in length. Two samples have a smooth saw-cut fault at 35 degrees (with respect to the axial axis), and one sample was fractured before testing to create a more natural rough fault (Figure 2). Many laboratory studies have shown that seismic velocity changes with applied stress**,** therefore the experiments in this study were performed under a fixed confined pressure to achieve a more representable stress scenario to fault reactivation in the subsurface. After reaching this stress scenario, the pore pressure was cyclically increased (Figure 1B).

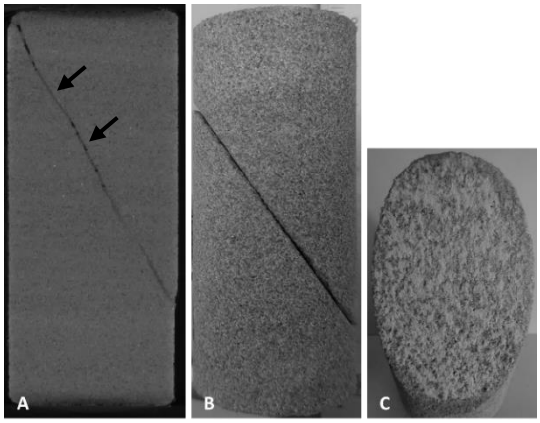

Figure 2*: Image of the faulted samples. A: A CT image of the fractured rock after reactivation experiment. The arrows point to areas of fault compaction or opening. B: Picture of the saw-cut faulted sample. C: Picture of the saw-cut fault plane, showing gouge formed on the fault plane.*

Examples

The micro-seismicity recorded from the reactivation of a saw-cut fault is shown in Figure 3, indicating a silent zone from the start of pore pressure reduction until fault reactivation. The fault instability and movement occur when, due to pore pressure increase, the effective normal stress drops, this is visible by a drop in the shear stress, indicating the stress release of the fault. After reactivation, the sharp drop in τ, the fault remains unstable until the fluid injection stops, visible by the generated micro-seismic events. Before the reactivation of the fault, two AE events are recorded, during the preparatory phase of the seismicity. Hence, with sensitive sensors, it is possible to record some precursory signals before the fault reactivation. Monitoring induced seismicity, however, still poses several challenges, including the need for near-real-time monitoring and limitations associated with seismic network quality (Grigoli et al., 2017).

The S-velocity change throughout the experiment is shown in Figure 1 along with the pore pressure cycles and does mostly follow the changing pore pressure. To investigate the more subtle changes, the derivative is plotted against the velocity change obtained by CWI and the K from CWD, both also showing the change between consecutive waveforms (Figure 4). A similar trend is visible in the velocity changes, the sharp drops in velocity clearly indicate the moment of reactivation. The magnitude of these drops increases per cycle, hence a larger stress drop (Figure 4A, C). Indicating the velocity change is a good proxy for the stress in the sample. The drop in $[dv/v]_{CWI}$ is more narrow, hence it gives a more accurate indication of both the preparatory phase and fault reactivation (Figure 4B).
Due to the smooth fault, stress release, thus fault reactivation is very rapid hence the preparatory phase is short. To reactivate the rough fracture more energy is needed, as some parts of the fracture aren't favorably oriented to move (Figure 2). During this extended preparatory phase, the drop in velocity is more clear (Figure 4D). Using CWD, the scattering coefficient K, a proxy for grain crushing or movement, is determined. This K clearly indicated the saw-cut fault reactivation, however, when the

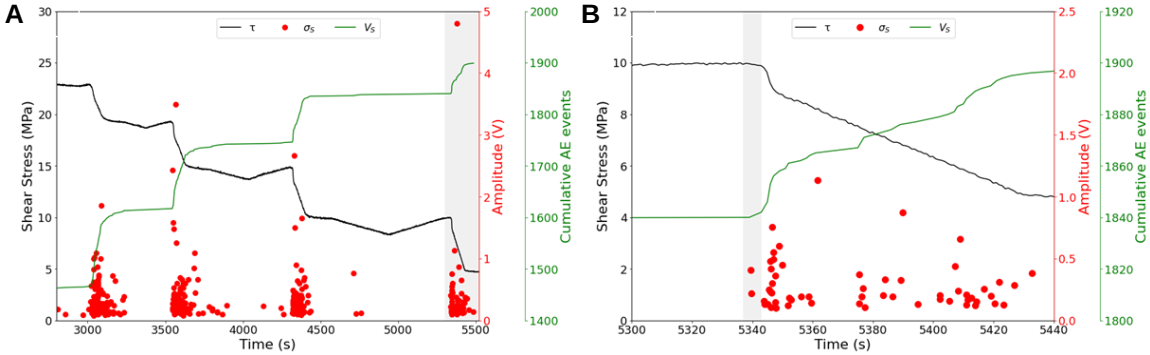

Figure 3: *Passive acoustic data (AE) during fluid cycling on a sample with a smooth saw-cut fault plane. Showing all the cycles in A and the 4th cycle and shaded the preparatory phase of fluid induced fault reactivation in B.*

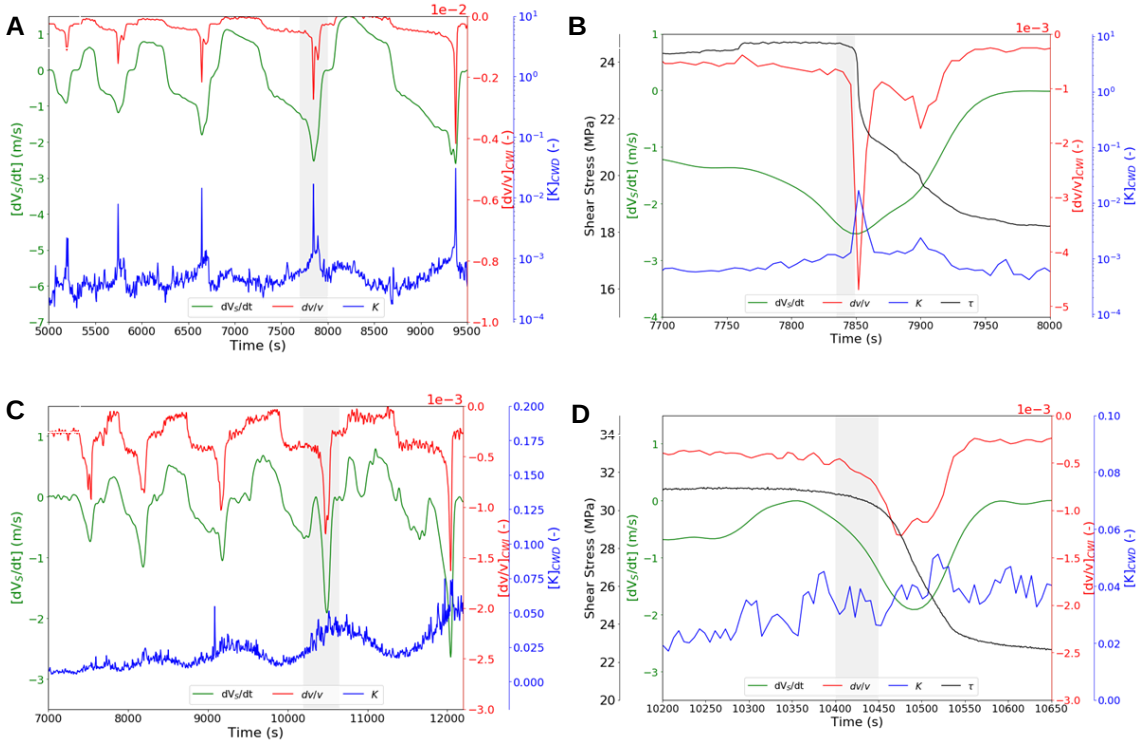

Figure 4: *Active acoustic data during fluid cycling. Showing the derivative of the S-wave velocity, velocity change from CWI and CWD scattering change K. A, B: results of reactivation of smooth saw-cut fault. A, B: results of reactivation of fracture. A and C showing all the cycles shown. B and D showing the 4th cycle, the preparatory phase of fluid induced fault reactivation is shaded.*

fault plane becomes more complex, the K seems to be of little use in detecting both the preparatory phase and fault reactivation (Figure 4C, D).

Conclusions

In this study, we used both active and passive monitoring techniques to detect the preparatory phase of an (induced) seismicity during the fluid-induced reactivation of faulted sandstones. We show that both techniques detect the preparatory phase of fault reactivation. Additionally, the precursory signals of the direct S-wave velocity, velocity obtained by CWI and K are compared for both a smooth saw-cut fault and a fracture. Showing the CWI velocity change is most sensitive to the preparatory phase and the fault reactivation. However, as all these are attributes obtained from the same wavelet a combination of these properties results in better detection of the preparatory phase of fault reactivation.

These results have shown that monitoring fault reactivation in the laboratory with active and passive techniques is feasible. As a result, the combination of passive and active techniques for monitoring and predicting stress changes could improve the prediction of induced seismicity.

Acknowledgements

We like to thank the laboratory staff of the TU Delft for their support. This research was (partially) funded by NWO Science domain (NWO-ENW), project DEEP.NL.2018.048

References

Barnhoorn, A., Verheij, J., Frehner, M., Zhubayev, A., and Houben, M. (2018). "Experimental identification of the transition from elasticity to inelasticity from ultrasonic attenuation analyses," *Geophysics* 83(4), MR221–MR229

Chiarabba, C., De Gori, P., Segou, M., and Cattaneo, M., (2020), Seismic velocity precursors to the 2016 Mw 6.5 Norcia (Italy) earthquake: *Geology*, v. 48, p. 924–928

Dempsey, D., & Suckale, J. (2017). Physics-based forecasting of induced seismicity at Groningen gas field, the Netherlands. *Geophysical Research Letters*, *44*(15), 7773–7782.

Grigoli, F. et al. (2017) 'Current challenges in monitoring, discrimination, and management of induced seismicity related to underground industrial activities: A European perspective', Reviews of Geophysics, 55(2), pp. 310–340.

Gulia, L., Wiemer, S., & Vannucci, G. (2020). Pseudoprospective evaluation of the foreshock traffic-light system in ridgecrest and implications for aftershock hazard assessment. *Seismological Research Letters*, *91*(5), 2828–2842.

Kaproth, B.M., Marone, C., (2013). Slow earthquakes, preseismic velocity changes, and the origin of slow frictional stick-slip. *Science* 341 (6151), 1229–1232.

Király-Proag, E., Zechar, J. D., Gischig, V., Wiemer, S., Karvounis, D., & Doetsch, J. (2016). Validating induced seismicity forecast models—Induced Seismicity Test Bench. *Journal of Geophysical Research: Solid Earth*, *121*(8), 6009–6029.

Larose, E., Planes, T., Rossetto, V., & Margerin, L. (2010). Locating a small change in a multiple scattering environment. *Applied Physics Letters*, *96*(20), 1–4.

Niu, F., Silver, P.G., Daley, T.M., Cheng, X., Majer, E.L., (2008). Preseismic velocity changes observed from active source monitoring at the Parkfield SAFOD drill site. *Nature* 454 (7201), 204–208.

Nur, A. (1971). Effects of stress on velocity anisotropy in rocks with cracks. *Journal of Geophysical Research*, 76(8), 2022–2034.

Shreedharan, S., Bolton, D. C., Rivière, J., & Marone, C. (2021). Competition between preslip and deviatoric stress modulates precursors for laboratory earthquakes. *Earth and Planetary Science Letters*, 553, 116623.

Snieder, R. (2006). The theory of coda wave interferometry. *Pure and Applied Geophysics*, *163*(2–3), 455–473.

Veltmeijer, A. & Naderloo, M. & Pluymakers, Anne & Barnhoorn, A.. (2022). Acoustic Monitoring of Laboratory Induced Fault Reactivation. *83rd EAGE Conference and Exhibition 2022*

Zotz-Wilson, R., Boerrigter, T., & Barnhoorn, A. (2019). Coda-wave monitoring of continuously evolving material properties and the precursory detection of yielding. *The Journal of the Acoustical Society of America*, *145*(2), 1060–1068.